

Nowcasting the lightning activity in Peninsular Malaysia using the GPS PWV during the 2009 inter-monsoons

Wayan Suparta^{1,*}, Ja'afar Adnan¹, Mohd. Alauddin Mohd. Ali²

¹ Universiti Kebangsaan Malaysia, Space Science Centre (ANGKASA), Institute of Climate Change, 43600 Bangi, Selangor, Malaysia

² Universiti Kebangsaan Malaysia, Department of Electrical, Electronic and System Engineering, Selangor, Malaysia

Article history

Received July 3, 2013; accepted March 19, 2014.

Subject classification:

GPS PWV, Lightning, SAFIR, Inter-monsoon, Nowcasting.

ABSTRACT

The spatial and temporal radio wave delay of the Global Positioning System (GPS) signal can be manipulated to estimate the precipitable water vapor (PWV) which favorable for meteorological applications. A rapid change of the water vapor amount was a precondition for the unbalanced atmospheric charges, which noticeably associated with the development of convective cloud as a lightning chamber. According to this fact, GPS derived PWV will be utilized to nowcasting the lightning event for the next couple of hours. The variances of PWV of four-selected station of the Peninsular Malaysia during the past two inter-monsoons events in May and November 2009 were analyzed. To clarify the response, the changes of PWV in hourly Δ (max-min) before the lightning event was investigated with minimum value 2 mm and is maintained at least three consecutive hours. There are 177 samples were extracted from this method and 69% of the sample showed the lightning occurrence with an average duration was after the six consecutive hours. The lightning day with 2 mm Δ was also higher than the fair weather of 6.3%. These findings suggest that the GPS data can be proposed further as a guide to nowcast the occurrence of lightning activity.

1. Introduction

Peninsular Malaysia is located at about 1°- 2° N of the equator line experiencing hot and humid climate throughout the year. The observation shows that, most of the areas closer to the equator generally have more lightning activity than the high latitude. This is due to the amount of sun radiations received by those areas together with huge water resources contribute to the large amount of evaporation that increases the water vapor in the troposphere. The measured water vapor known as precipitable water vapor (PWV) is defined as the height of liquid water that would result from condensing all the water vapor in a column from the sur-

face to the top of the atmosphere [Coster et al. 1996]. PWV is also the most important of the greenhouse gases in the atmosphere and determines the Earth's climate. By monitoring a long-term PWV and accurate quantification of their changes can help to detect and predict the earth's climate variability such as a lightning. There are a few options of water vapor measurements have been recently conducted such as through satellite observations, radiosonde, water vapor radiometer (WVR) and global positioning system (GPS). The recovery of the water vapor by satellites is problematical over the land due to the inconsistency of the surface temperature. Radiosonde network is costly to operate whereas the data gathered is only twice daily that constraint to observe rapid changes of the water vapor with the position and time. Another option is a WVR measurement that operates in the thermal infrared, which very sensitive to any stray light from ambient sources, therefore, careful attention is required to the systematic errors that can occur through the calibration process. The recent technology, GPS can provide a continuous measurement close to a real-time basis of moisture around the site. The installed GPS receiver can be configured to log a continuous data automatically with a reasonable cost and precise data with a high temporal and spatial resolution. According to Nakamura [2003], the low-cost ground based GPS sensing technique has sufficient accuracy for practical use in nowcasting of weather, which is capable to estimate PWV up to 1 mm accuracy with about 90-95% of reliability compared to the radiosonde and WVR. Furthermore, the near real-time GPS column water vapor using predicted orbit agrees with radiosondes and

MWR within 2 mm rms [Rocken et al. 1997].

Water vapor is a source of convective clouds, and its distributions have largely affected the formation and development of the convective precipitation systems. Price [2000] noted that the variability of water vapor amount in the tropospheric cavity is associated with the existence of lightning. In addition, Inoue and Inoue [2007] observed in the active thunderstorm days show the distinct diurnal of PWV variation. In similar work, the PWV was observed to increase during the lightning event and lower compared to the day without lightning [Suparta et al. 2011]. The knowledge in cloud electrification and discharging processes is crucial to determine the connection between the PWV and the lightning. [Backer et al. 1999, Williams 2003, Zipser and Lutz 1994 and Ziegler et al. 1991] have unanimously stressed the strength of vertical updraft was a core factor that will determine the effective charge separation in the cloud to produce lightning.

This work aims to discover the possibility for nowcasting the lightning activity throughout the changes in the GPS signals using the PWV observation. The expansion of GPS receiver as well as the antenna technology facilitates a cost effective technique for monitoring the tropospheric phenomenon on a global basis. The widening of GPS network across the continents facilitates the superb temporal and spatial resolution, which promises the high accuracy detection system. The result from lightning inferred from GPS has a potential to improve the nowcasting and weather forecasting. In this paper, we observed the characteristic features of the GPS PWV associated with the lightning activities that occurred during the beginning of summer and winter monsoon (May and November) of 2009. The relationship between the water vapor and convective activities were also discussed quantitatively.

2. Material and methodology

2.1. Materials

The GPS and meteorological data from four selected stations were used in this study where the location is shown in Figure 1. The stations were located at Kuala Krai, Kelantan (KRAI), Mersing, Johor (MERS), Bandar Muadzam Shah, Pahang (MUAD) and Universiti Kebangsaan Malaysia, Bangi, Selangor (UKMB). KRAI, MERS, MUAD and UKMB stations were located at about northeast, southeast, center and west part of the Peninsular Malaysia, respectively.

The three stations other than UKMB were belonged to Department of Survey and Mapping Malaysia (DSMM) which connected to Malaysia Real-Time Kinematic (MRTK) GNSS Network. The station used the Trimble TS5700 for MERS station, while both

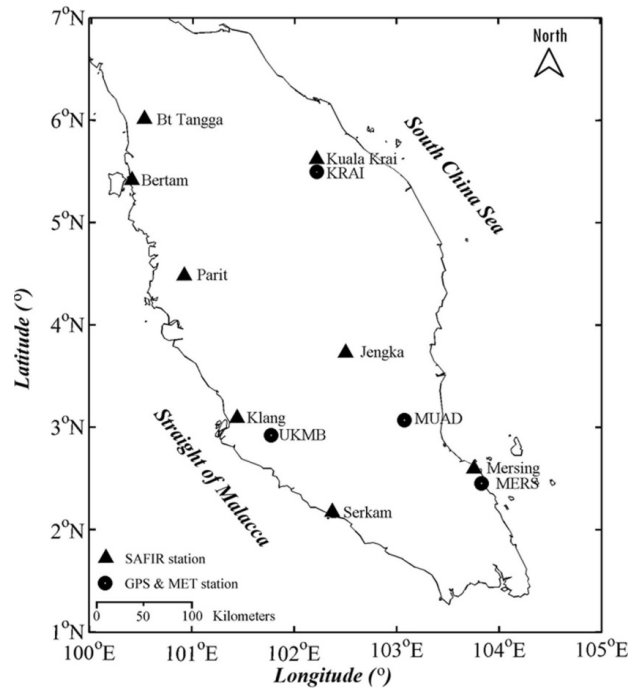


Figure 1. Location of GPS, meteorology and lightning sensors over the Peninsular Malaysia.

KRAI and MUAD were used the Trimble NetR5. The systems were configured to log the GPS data in every 15 seconds. UKMB station belonged to the Space Science Centre (ANGKASA), Universiti Kebangsaan Malaysia, which used the Trimble TS5700 GPS receiver. The system was configured to record the GPS data at 5 seconds resolution. The detail locations of GPS receiving system used in this work were shown in Table 1.

At UKMB, the surface meteorological data have been logged using the MET3A sensors produced by Paroscientific, Inc., USA. The system measured the surface pressure (mbar), temperature ($^{\circ}\text{C}$) and relative humidity (%). Each parameter was logged in a 4 second interval. The Malaysian Meteorological Department (MMD) supported the meteorological data for KRAI, MERS and MUAD stations with one-minute intervals.

In addition to GPS and meteorological data, lightning data were required as a comparison to detect the lightning activity between the Earth's surface and the upper troposphere. The lightning occurrence then can be inferred from the PWV changes. To establish the pattern of GPS PWV changes due to lightning events, the *Surveillance et Alerte Foudre par Interférométrie Radioélectrique* (SAFIR) was employed. The system has the capability to detect and record all the lightning events such as inter-cloud (IC) and cloud-to-ground (CG) activities as well as the strength of the electrostatic charge (in kA). Eight SAFIR sensors have been installed throughout Peninsular Malaysia as shown in Figure 1. Detail of the sensor location is listed in Table 2. The system belongs to MMD used the SAFIR3000 model. The base of

| No. | Station | Latitude (°N) | Longitude (°E) | Height (m) | Receiver type |
|-----|---------|---------------|----------------|------------|----------------|
| 1 | KRAI | 05° 30' 07" | 102° 13' 11" | 31.77 | Trimble NetR5 |
| 2 | MERS | 02° 27' 12" | 103° 49' 44" | 18.10 | Trimble TS5700 |
| 3 | MUAD | 03° 04' 18" | 103° 04' 27" | 50.10 | Trimble NetR5 |
| 4 | UKMB | 02° 55' 23" | 101° 46' 23" | 35.64 | Trimble TS5700 |

Table 1. GPS Coordinates for KRAI, MERS, MUAD and UKMB stations.

| No. | Station | Latitude (°N) | Longitude (°E) |
|-----|----------------------|---------------|----------------|
| 1 | Bt. Tangga, Kedah | 05° 23' 00" | 100° 33' 00" |
| 2 | Kuala Krai, Kelantan | 05° 32' 03" | 102° 11' 55" |
| 3 | Bertam, Penang | 05° 25' 05" | 100° 18' 30" |
| 4 | Parit, Perak | 04° 29' 29" | 100° 55' 09" |
| 5 | Jengka, Pahang | 03° 44' 29" | 102° 32' 37" |
| 6 | Klang, Selangor | 03° 02' 38" | 101° 26' 27" |
| 7 | Serkam, Melaka | 02° 09' 00" | 102° 22' 59" |
| 8 | Mersing, Johor | 02° 26' 08" | 103° 49' 58" |

Table 2. Location of SAFIR 3000 sensors over the Peninsular Malaysia.

the system is located in Petaling Jaya, Kuala Lumpur and the control station is located at Kuala Lumpur International Airport (KLIA).

2.2. Methodology

The method employed in this study was based on the concept of the signal propagation delay. The GPS signals will propagate in a curve due to variations in the refractive index caused by the high density medium when the signal passes through the ionosphere and troposphere. The ionosphere is a dispersive medium that bends the GPS radio signal and changes its speed as it passes through the various ionospheric layers to reach the receiver. At this layer, the delay is proportional to the number of free total electron content (TEC) [Garner et al. 2008]. The ionospheric delay was properly modeled and can be removed using the linear combination of L1 and L2 carrier-phase measurements, whereas the troposphere is a nondispersive medium in the radio frequency below 15 GHz [Hay and Wong 2000]. Consequently, the tropospheric delay of the GPS carriers and codes are identical, which causes the satellite-to-receiver range will be longer than the actual geometric range [El-Rabbany 2002]. The whole traveling delay is associated with the refractive index of the troposphere that reflected in the amount of PWV along the signal path. This delay depends on the temperature (T), surface pressure (P) and relative humidity (RH), above the Earth’s surface. Thus, the availability of T, P

and RH together with GPS data (observation and navigation) at the particular location allowed the measurement of GPS PWV as illustrated in Figure 2. GPS PWV represents the zenith tropospheric delay (ZTD) and zenith hydrostatic delay (ZHD). The PWV was estimated from zenith wet delay (ZWD) that the product of subtracting the ZHD from ZTD. The detail of the GPS PWV determination for this study can be referred in Suparta et al. [2008]. The lightning activities are expected nowcast from the variation of PWV response.

The data processing and analysis programs were written in Matlab, using the Tropospheric Water Vapor Program (*TroWav*) [see Suparta et al. 2013]. In this study, the accuracy of PWV derived from ground-based GPS meteorology depends on three major factors known as orbital error, pressure error and temperature error. The orbital errors was attached in determining the satellite elevation angle by using the IGS ultra-rapid orbit prediction to minimize the impact of predicted orbit errors on ZTD estimates [Ge et al. 2012]. The pressure errors occurred in determination of ZHD, which correlated with GPS coordinates. In this case, the assessment of the accuracy coordinates used the International terrestrial reference frame, ITRF2002 coordinates [Altamimi et al. 2002]. The temperature error was occurred in the estimation of weighted mean temperature to convert the ZWD into PWV. We used the surface temperature measured at the site to minimize the factor conversion error. On the other hand, for the error asso-

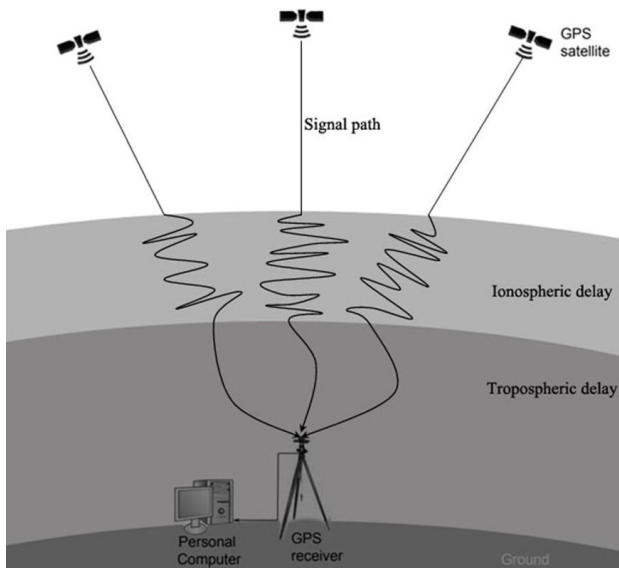


Figure 2. The illustration of how GPS signal can be used to sense the lightning activities through GPS PWV.

ciated with pressure and temperature sensors, we can eliminate by using well-maintained equipment and practice proper procedures for data collection. By handling of all the above errors, the accuracy of PWV determination is capable used to relate the lightning activities.

2.3. Data processing

The analysis was concentrated on the GPS PWV variation that occurs before the first discharge of the lightning series. In this work, the summary of the lightning detection method is depicted in Figure 3. From the figure, both GPS data (observation and navigation) in *.dat files were converted into Receiver Independent Exchange Format (RINEX). The process was using the freeware toolkit known as the Translate/Edit/Quality Check (TEQC) developed by UNAVCO (<http://www.unavco.org>). A 30 second data sampling has been set for a reasonable processing time as well as to avoid the processor problem. At the last stage

of PWV determination, the maximum elevation angle together with surface meteorological data set was prepared at a one-minute interval. Note that, the data interval processed was depending on the resolution of both GPS and surface meteorological data intervals.

For SAFIR, the raw data was in ASCII format that consisted of IC and CG lightning, detection accuracy up to millisecond, the coordinates of the event and the strength of electric charge. Data were recorded based on the lightning occurrences that cover throughout the Peninsular Malaysia, Singapore and the eastern part of Sumatra Island. Figure 4a,b shows the example of heavy lightning days that occurred over the Peninsular Malaysia. From the figure, the blue and red dot shows the IC and CG discharged respectively. In this work, only lightning data occurred within 20 km radius from GPS station was selected. The mixed data of IC and CG events were compiled separately into one-minute resolution. However, due to the limited of GPS and meteorological data, only the event during the beginning of the summer monsoon (May) and at the beginning of winter monsoon (November) of 2009 were analyzed. Both the monsoon periods are called the inter-monsoons. In addition, the SAFIR network in Malaysia was deployed in late 2008, and the data ready for the public was started in May 2009.

3. Results

3.1. Lightning activity at four selected stations

Table 3 shows the distribution of lightning activity during the 2009 inter-monsoons. During both inter-monsoons periods, the lightning activity was observed highest at UKMB station followed by MUAD and MERS stations and the lowest is at KRAI station. The difference in the amount of lightning activity at UKMB (highest) and KRAI stations (lowest) during the period of the first and second inter-monsoon was 28,172 and 77,649 respectively.

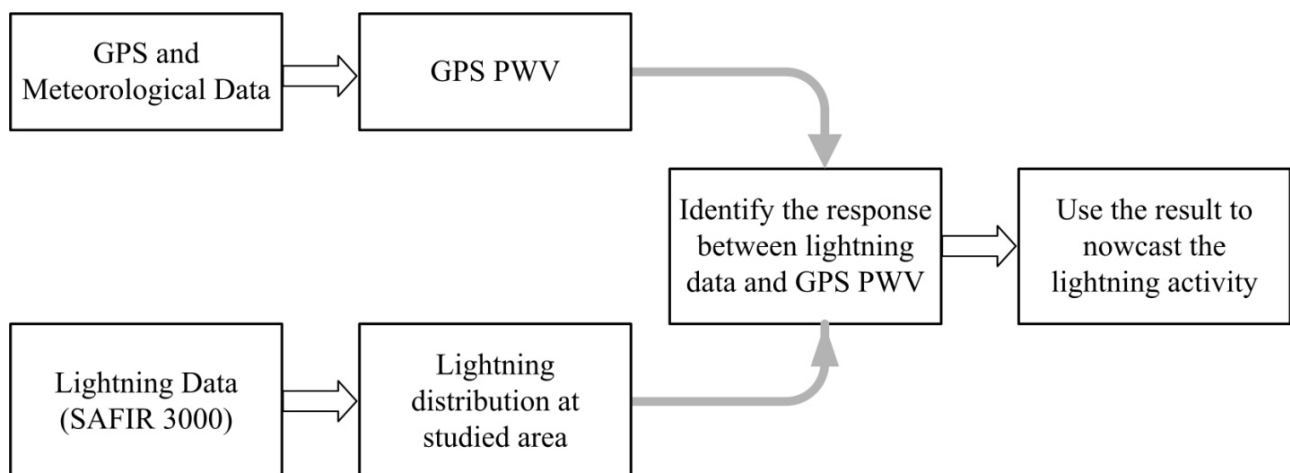


Figure 3. Summary of the processing methodology.

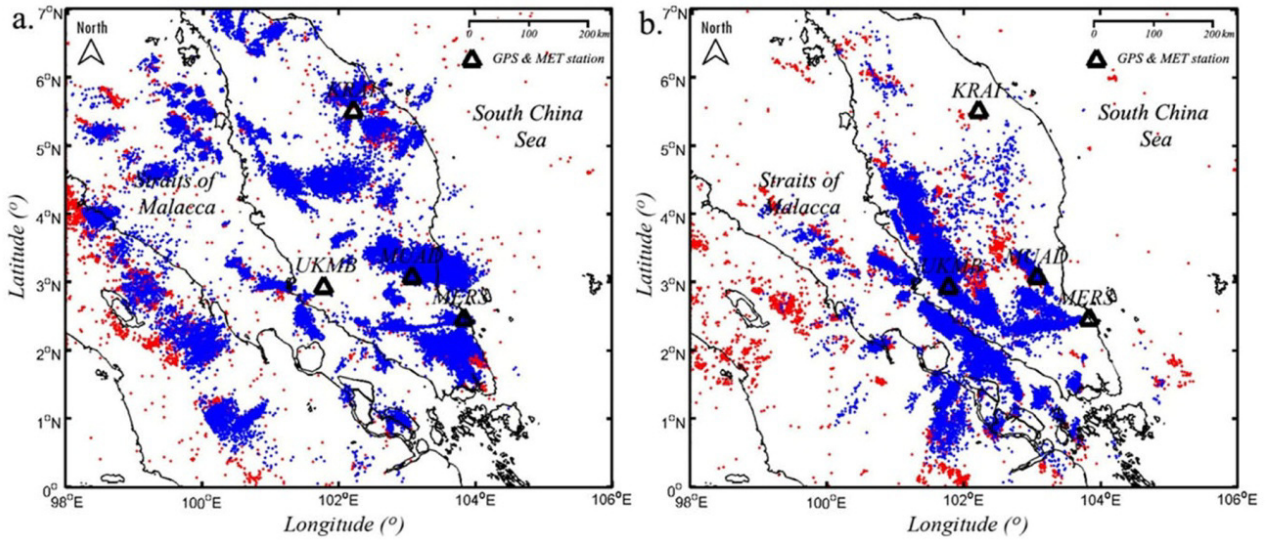


Figure 4. Examples of the heavy lightning days over the Peninsular Malaysia during (a) May 1st, 2009, and (b) November 7, 2009.

The amount of lightning activity at UKMB station during the second inter-monsoon was about three times greater than the first inter-monsoon. This scenario was about 27, 24 and 7 times lower during the second inter-monsoon compared to the first inter-monsoon for KRAI, MERS and MUAD stations, respectively. For both inter-monsoons, the number of IC lightning is always higher than the number of CG lightning, while the number $-CG$ lightning was higher than $+CG$ lightning. However, the ratio of the IC: CG and $-CG$: $+CG$ during both inter-monsoons respectively was found changeable.

Figures 5 and 6 showed the distribution of lightning activity at the four selected stations during the first and second 2009 inter-monsoons. The figures clearly show that the amount of lightning activity at KRAI, MERS and MUAD stations were found high in the first inter-monsoon compared to the UKMB situation which is high in the second inter-monsoon. In general, the lightning ac-

tivity is more frequent in the afternoon, especially between 12:00 LT and 22:00 LT (see the shaded area). The lightning activity is rare in the morning and after 22:00 LT. This character will be discussed in the next section.

3.2. GPS PWV variations during inter-monsoons period

The GPS PWV variation during the first and second inter-monsoons period at four selected stations in one-minute intervals are presented in Figures 7 and 8, respectively. PWV data at the certain days could not be generated due to the unavailability of GPS or meteorological data, especially for UKMB station. The PWV for each station was observed similar variations with a low in the morning from 00:00 LT to 08:00 LT, a gradual increase after 08:00 LT until reaching a maximum during the afternoon from 12:00 LT to 17:00 LT and a slow decrease in the evening. During the first inter-monsoon period, the variations of GPS PWV at all stations were

| Inter-monsoon | Station | Total IC | CG | | | | IC:CG | Total lightning |
|---------------------------|---------|----------|-------|-------|-------|-------|-------|-----------------|
| | | | -CG | +CG | Total | Ratio | | |
| First (May 2009) | KRAI | 6,998 | 1,001 | 398 | 1,399 | 2.52 | 5.00 | 8,397 |
| | MERS | 27,848 | 1,674 | 340 | 2,014 | 4.92 | 13.83 | 29,862 |
| | MUAD | 33,001 | 2,276 | 722 | 2,998 | 3.15 | 11.01 | 35,999 |
| | UKMB | 34,222 | 1,888 | 459 | 2,347 | 4.11 | 14.58 | 36,569 |
| Second (November 2009) | KRAI | 195 | 72 | 34 | 106 | 2.12 | 1.84 | 301 |
| | MERS | 1,091 | 128 | 22 | 150 | 5.82 | 7.27 | 1,241 |
| | MUAD | 5,050 | 184 | 66 | 250 | 2.79 | 20.2 | 5,300 |
| | UKMB | 72,867 | 4,031 | 1,052 | 5,083 | 3.83 | 14.34 | 77,950 |

Table 3. Lightning activities during the 2009 inter-monsoons.

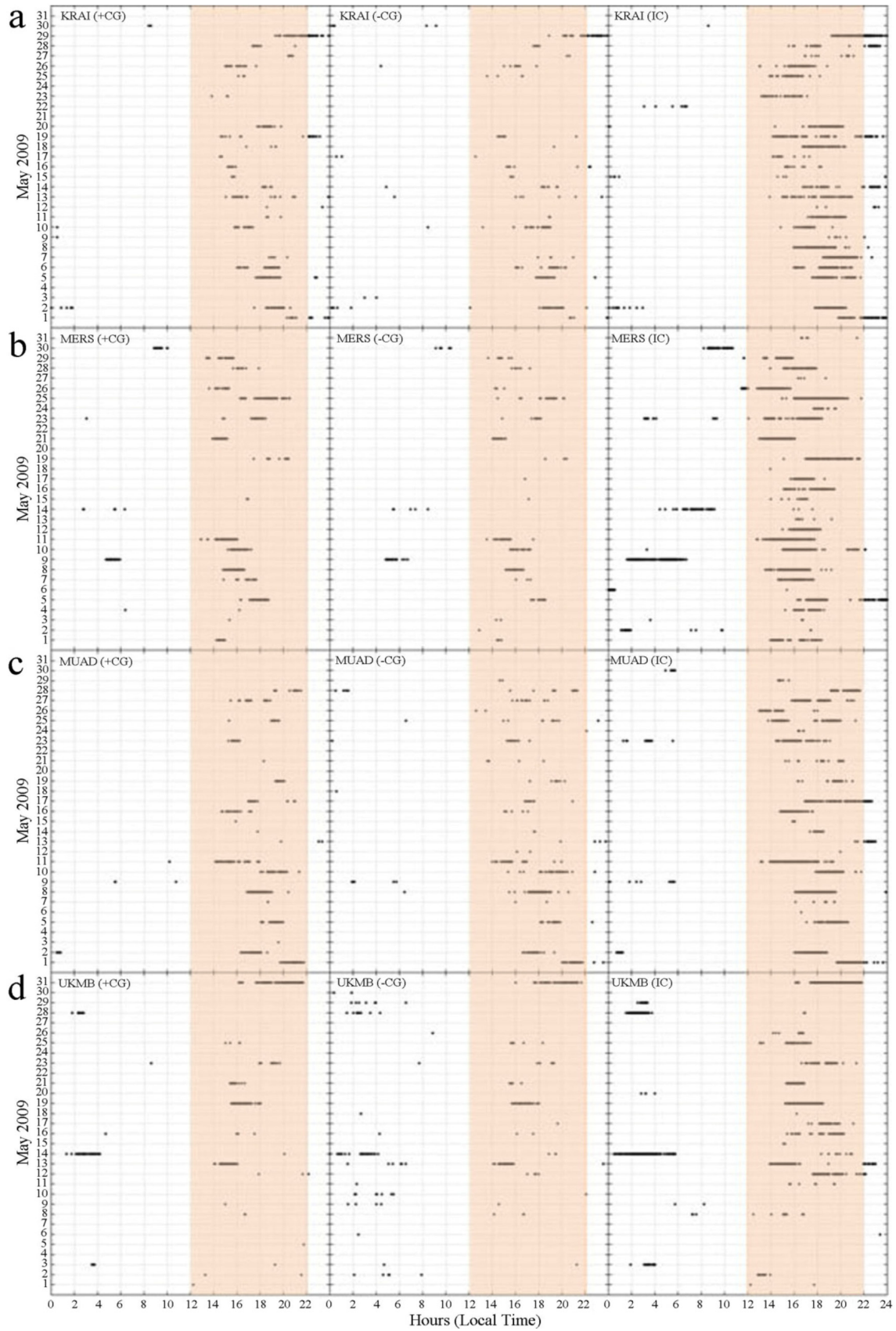


Figure 5. Lightning distribution at four selected stations during the first pre-monsoon (May 2009).

mainly consistent with only three short irregular variations (shaded by grey colour and labeled as **i**, **ii** and **iii**). For area **i**, the irregular variation has been clearly observed for MERS and MUAD stations, where the PWV

peak is lower than the previous and following days. However, the lowered of PWV peak at KRAI was lasted for three days from May 3 to 5, 2009, but only the signal for May 3 has been highlighted since the regular varia-

NOWCASTING THE LIGHTNING ACTIVITY

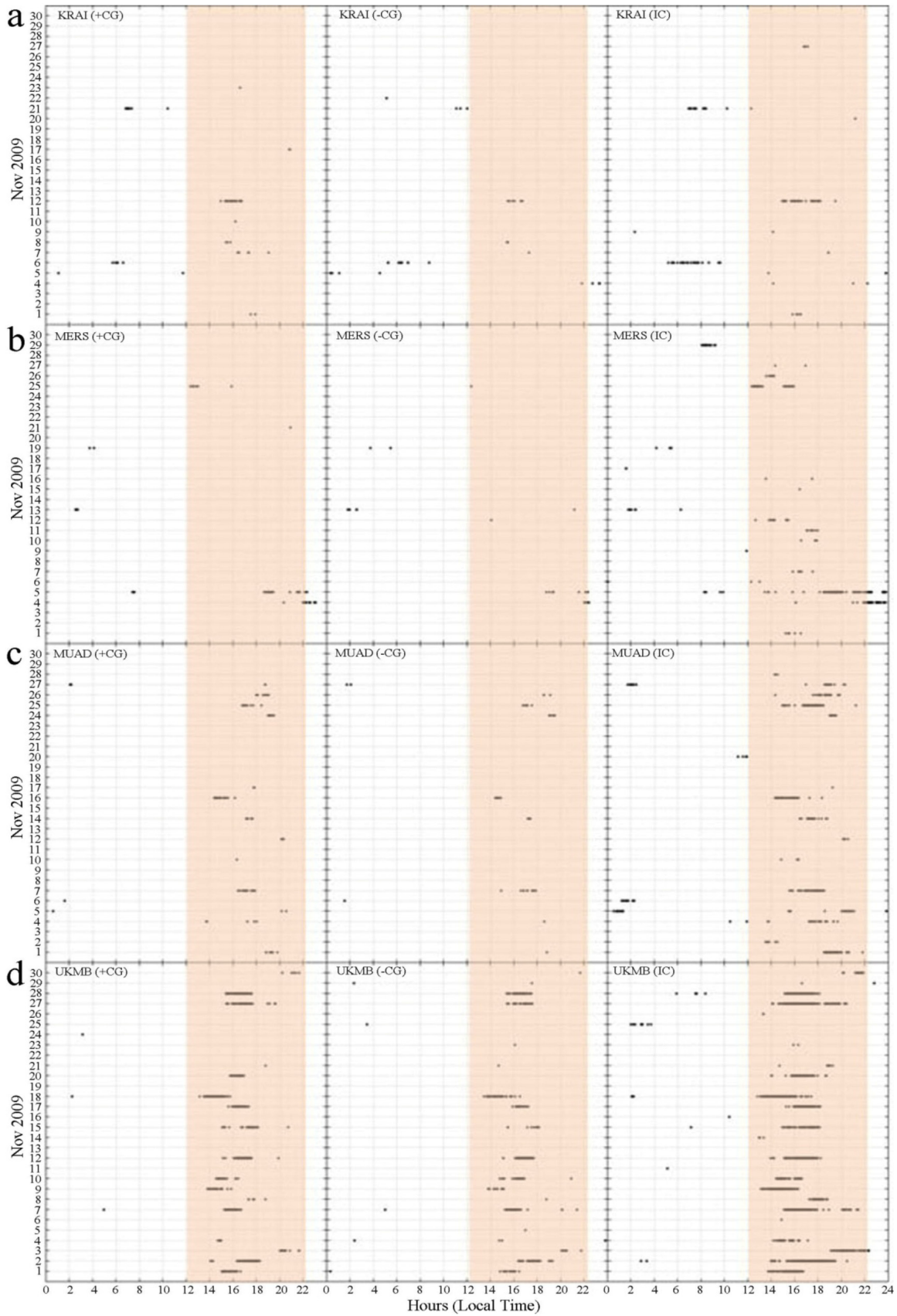


Figure 6. Lightning distribution at four selected stations during the first pre-monsoon (November 2009).

tion on May 4 and 5 was occurred at the other three stations. This scenario can be correlated with the initiated of a tropical storm over the south China Sea, known as the Emong (Chan-Hom) and moving from the centre

of south China Sea to Philippine islands (<http://www.typhoon2000.ph/season09s.htm>). The irregular variation for UKMB was not clear since the location was at the west part of peninsular. For area ii, the PWV varia-

tion was observed regular at KRAI and irregular for MERS, MUAD and UKMB. The signals for both MERS and MUAD stations were lower than the previous and following days. In contrast, the signal peak at UKMB was the highest for the month. For area *iii*, the signal was irregular at MERS and MUAD stations and found missing for the UKMB station. MERS station was recorded the highest standard deviation (STD) value, smoothed signal at MUAD and regular signal for KRAI. For both areas *ii* and *iii*, there is no extreme weather phenomenon has been detected. However, variations in the temperature and relative humidity were strongly noticed as the initiation of the atmospheric instability nearby the area, especially in the south China Sea.

For the second inter-monsoon period, the PWV variation was changeable (labeled as *iv* and *v*). For both inter-monsoons, the irregular variations were due to the extreme weather phenomenon such as tropical storm, which can be associated with a low or no lightning activity. The average of GPS PWV variation for a normal weather with lightning activity and for extreme weather during both inter-monsoons was plotted in Figure 9. In both scenarios, the PWV was started to increase at about 07:00 LT and marked with 'a' and 'c'. The maximum (marked with 'b' and 'd'), average and minimum of PWV values were observed almost the same of about 48 mm, 47 mm and 45 mm, respectively. Two significant characters that have been observed from these

two conditions were about the total increment of PWV and the total duration, which required reaching the peak point. The increment of PWV average during the normal weather with lightning was 0.75 mm/hr, which is 0.22 mm/hr faster than during the extreme weather condition. Meanwhile, the total increment of PWV average for extreme weather was 4.04 mm, which is 0.64 mm higher compared to the normal weather. The figure also showed that, the fluctuation of PWV represented by the STD during the extreme weather was 1.16 mm, which is 0.2 mm higher than the STD during the normal weather with lightning.

During the first inter-monsoon period, the range of the PWV mean at all stations varied from 5 mm to 10 mm, with the exception of the value at MUAD, which was approximately 4 mm. In contrast, the range during the second inter-monsoon period was smaller (less than 5 mm), with the exception of the range at MUAD, which was approximately 3 mm. The GPS PWV variation during both of inter-monsoon periods is summarized in Table 4. The average GPS PWV value during the first inter-monsoon period was higher than in the second inter-monsoon period with the exception at the UKMB station. This fluctuation during both inter-monsoons periods is indicated by a delta (Δ). The difference in the Δ value between the two inter-monsoon periods varied between 1.17 mm and 2.5 mm. The highest Δ values were observed at MERS station at 10.77 mm and

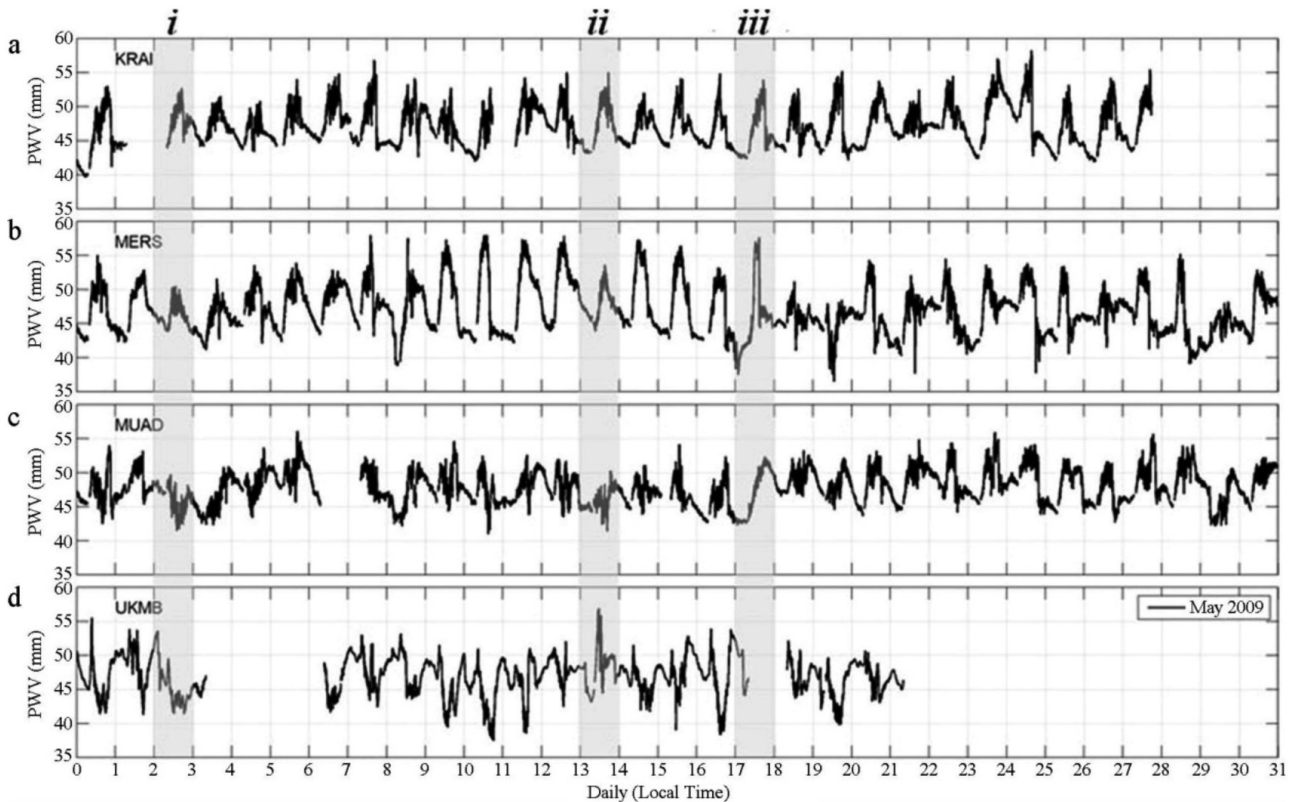


Figure 7. GPS PWV variation during the first inter-monsoon at four selected stations.

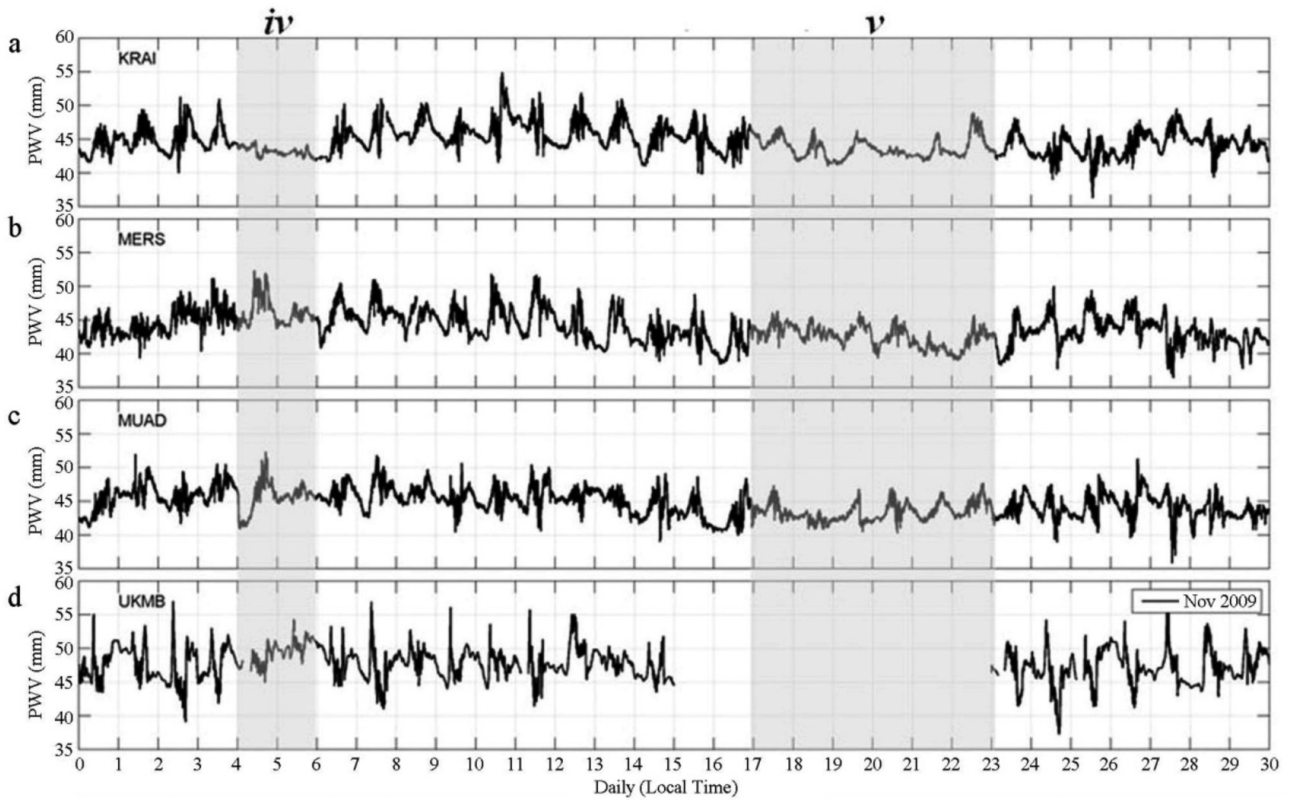


Figure 8. GPS PWV variation during the second inter-monsoon at four selected stations.

8.27 mm for first and second inter-monsoon periods, respectively. This variation is similar to the STD values observed during the first inter-monsoon, which was higher than in the second inter-monsoon period with a value varying from 0.25 mm to 0.59 mm.

4. Discussion

4.1. The response of GPS PWV on lightning activity

To identify the response of PWV on lightning event, both daily lightning activity (CG and IC) and PWV were plotted together. As an example, changes of PWV that possibly associated with lightning activi-

ties were shown in Figures 10 and 11. In the lightning data, the IC and CG were represented by yellow and black bar graphs, respectively. Note that, the unit shown on the Y-axis was only for CG. From the same figure, the PWV was plotted in hourly basis to enable the calculation of Δ (max-min) and STD. The Δ of PWV was represented by a red error bar (solid line) that refers to the Y-axis on the left. To strengthen the finding, the STD was used to validate the results of Δ as shown by the dashed line that refers to the Y-axis on the right side. Note that the data gap from 07:00 LT to 09:00 LT in Figure 10 was identified due to the missing of GPS data at KRAI station.

| Inter-monsoon | Station | Average value (mm) | | | | |
|-----------------------|---------|--------------------|-------|---------|--------------------|------|
| | | Maximum | Mean | Minimum | Δ (max-min) | STD |
| First (May 2009) | KRAI | 52.11 | 47.06 | 43.18 | 8.92 | 2.07 |
| | MERS | 51.61 | 46.90 | 40.84 | 10.77 | 2.67 |
| | MUAD | 51.67 | 47.81 | 43.25 | 8.42 | 2.20 |
| | UKMB | 51.76 | 46.85 | 42.87 | 8.9 | 2.36 |
| Second (Nov. 2009) | KRAI | 48.80 | 44.60 | 41.54 | 7.27 | 1.75 |
| | MERS | 47.79 | 43.79 | 39.52 | 8.27 | 2.08 |
| | MUAD | 47.97 | 44.59 | 40.92 | 7.05 | 1.81 |
| | UKMB | 51.55 | 47.57 | 43.82 | 7.73 | 2.11 |

Table 4. The comparison of GPS PWV during two inter-monsoons at four selected stations.

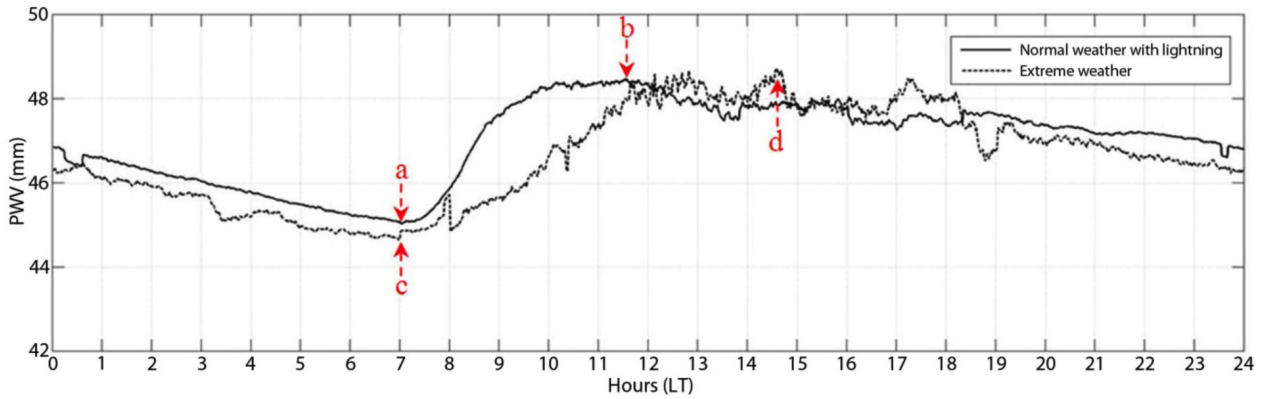


Figure 9. GPS PWV average for normal weather with lightning and extreme weather, where ‘a’ and ‘c’ are the starting points, and ‘b’ and ‘d’ are the peak points.

The impacts of Δ during the lightning and fair weather condition for 2009 inter-monsoons are compiled in Table 5. There are 215 lightning days from 244 days of both inter-monsoons (May and November 2009) at four-selected stations were analyzed. The balance of 21 and 8 days for the first and second inter-monsoons respectively was missing data. The rest is no lightning or called fair weather. In the result, the samples were grouped into two categories labeled as **A** for the Δ greater than 2 mm ($\Delta \geq 2$ mm), and category **B** for the Δ less than 2 mm ($\Delta < 2$ mm). Then, the samples in each category were grouped into lightning day and fair weather day as shown in Table 5. As a result, the total samples with $\Delta \geq 2$ mm was about 89% (92 days) and 76% (85 days) for the first and second inter-monsoons, respectively. From that number, 80% (74 days) and 56% (48 days) for the first and second inter-monsoons respectively were the lightning days. As a summary, about 82% (177 days) of the samples was the day with the $\Delta \geq 2$ mm and about 69% of them was a lightning day.

The duration of lightning development was estimated from the first $\Delta \geq 2$ mm until the first lightning discharged. For example, the duration of the lightning development for May 1st at KRAI and November 7 at MUAD was about 11 hours and 7 hours, respectively (see Figures 10 and 11). The compilation of daily lightning development period was used to estimate the lead-time before the lightning occurrence as shown in the sixth column of Table 5. From the table, the beginning of lightning for both inter-monsoons was about 6 hours.

Table 5 also showed the comparison of Δ and STD averages for the overall samples, lightning day and fair weather in the seventh to twelfth column. In the first inter-monsoon, Δ for the fair weather was higher of 1.5 mm and 0.1 mm than the overall and the lightning day, respectively. The same trend was observed for STD during fair weather which higher of 0.36 and 0.1 mm than the overall and the lightning day, respectively. In contrast, during the second inter-monsoon, Δ for the lightning day was higher of 1.9 mm and 0.6 mm than the overall and the

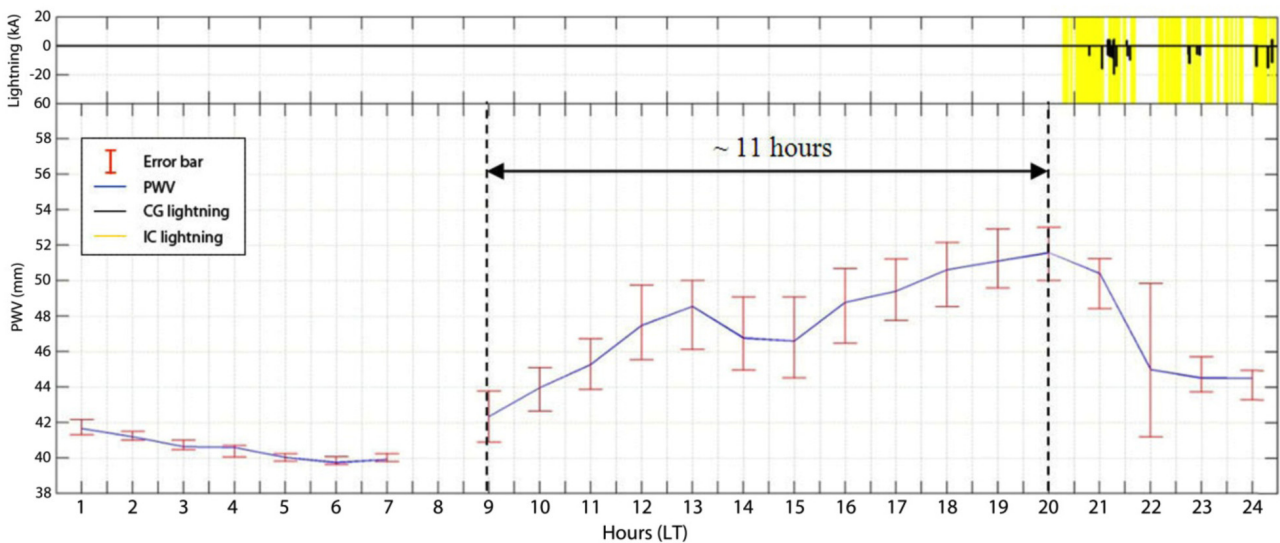


Figure 10. The variation of PWV during heavy lightning on May 1st, 2009, for KRAI station. The top panel of the figure showed the lightning activity and the bottom showed the PWV variation together with error bar graph.

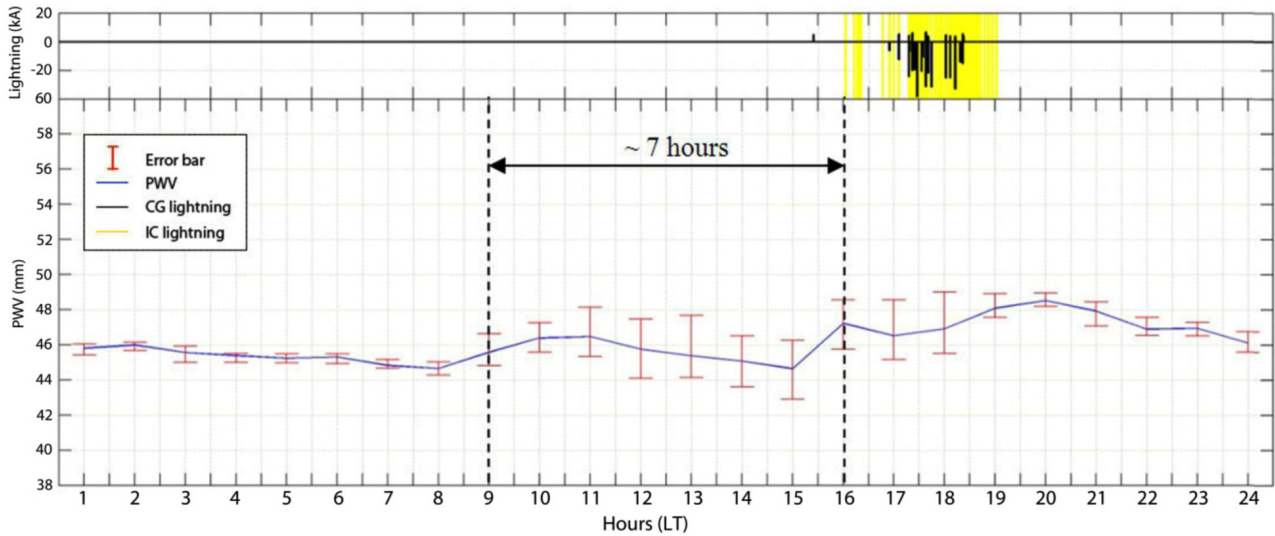


Figure 11. The variation of PWV during heavy lightning on November 7, 2009, for MUAD station, which similar presented as Figure 10.

fair weather, respectively. For both inter-monsoons, the Δ for the lightning day was 45% and 6.3% higher than the Δ for overall and fair weather, respectively.

4.2. Proposed mechanism of nowcasting

The information of Δ at few hours before the lightning was very important. The Δ of PWV acts as an indicator of water vapor instability in the atmosphere that can be associated with the lightning occurrence.

The observation during the inactive sun radiation period (00:00 LT to 07:00 LT) resulting majority of Δ , which found less than 2 mm, and it can be associated with the weakness of physical transformation between the water vapor and water particles in the troposphere. Thus, the sun radiation was detected as a key factor of this phenomenon. For nowcasting purpose, the minimum lead-time of three hours before the lightning is sufficient for the people to seek the shelter after the ac-

| | | A ($\Delta \geq 2\text{mm}$) | | B ($\Delta < 2\text{mm}$) | | PWV (mm) * | | PWV STD (mm) * | | | | | |
|---------|------|--------------------------------|--------------|-----------------------------|--------------|---|---------|----------------|--------------|---------|-----------|--------------|------|
| | | Lightning | Fair weather | Lightning | Fair weather | Period (hours) ($\Delta > 2\text{mm}$) | Overall | Lightning | Fair weather | Overall | Lightning | Fair weather | |
| May | KRAI | 26 | 22 | 4 | - | - | 6.3 | 2.24 | 3.76 | 3.39 | 0.58 | 0.89 | 0.83 |
| | MERS | 31 | 22 | 4 | 5 | - | 5.9 | 2.29 | 3.67 | 4.07 | 0.60 | 0.92 | 1.10 |
| | MUAD | 30 | 22 | 7 | - | 1 | 6.5 | 2.26 | 3.49 | 3.51 | 0.56 | 0.83 | 0.83 |
| | UKMB | 16 | 8 | 3 | 4 | 1 | 5.1 | 1.97 | 3.36 | 3.74 | 0.53 | 0.86 | 0.97 |
| Nov. | KRAI | 30 | 7 | 13 | 2 | 8 | 5.0 | 1.60 | 4.01 | 3.80 | 0.42 | 0.97 | 0.93 |
| | MERS | 30 | 11 | 11 | 2 | 6 | 6.6 | 1.89 | 3.41 | 3.31 | 0.49 | 0.83 | 0.84 |
| | MUAD | 30 | 15 | 9 | - | 6 | 6.3 | 1.80 | 3.55 | 3.51 | 0.46 | 0.90 | 0.84 |
| | UKMB | 22 | 15 | 4 | 2 | 1 | 6.0 | 1.96 | 3.83 | 1.96 | 0.50 | 0.98 | 1.08 |
| Average | | 26.88 | 15.25 | 6.88 | 3 | 3.83 | 5.96 | 2.00 | 3.64 | 3.41 | 0.52 | 0.90 | 0.93 |

* Δ and STD are for PWV values, respectively.

Table 5. The impact of PWV during the lightning and fair weather conditions for 2009 inter-monsoons.

tivation of the early warning system. In this work, the Δ minimum was set at least 2 mm and maintained within three consecutive hours before the lightning event. Only the case with this criterion will be associated with the progress development of convective cloud can be used in nowcasting the lightning event.

The mechanism of nowcasting is proposed in Figure 12, where the first process is involved the evaporation, labeled as 'A'. This process will change the physical form of water from liquid to vapor. The rate of evaporation of water depends on the surface temperature, the pressure and the humidity. The warm air will move upward until the cloud high and cold water will move downward as compensation. The movement at high altitude will reduce the temperature of water vapor up to the freezing stage (0°C), which causes the water vapor condenses (B) into the ice particles, graupel and tiny water droplet to forming the cloud, which reduce the water vapor. The significant decrease in PWV can be associated with the existence of a sudden cold surged following by drastic cloud formation also known as the convective cloud formation. During lightning days, the high value of Δ ($>2\text{mm}$) was shown that the PWV has experienced a physical transition between vapor state and solid state, which much faster than the overall condition and during the fair weather, as shown in the results. In this study, the Δ must maintain for at least three consecutive hours before can be associated with the development of lightning activity. The average period of

lightning development before the first lightning discharge is six hours. PWV decreased was due to the physical transition of water vapor to ice particles (solid state) that will increase the size of the convective clouds. In contrast, the reversion process of warm air will increase the PWV. This process usually compliments with the heavy vertical air motion, which causes large charge separation (D). The expansion of the convective cloud will increase the potential difference that caused a strong lightning. In addition, the convective cloud is also associated with precipitation (C) such as rainfall, snow and hail.

5. Conclusion

The variances of GPS PWV and their response with the 215 samples of two inter-monsoons in 2009 were analyzed to demonstrate the potential use of the GPS PWV to nowcasting the lightning occurrence. Three significant findings can be emphasized from this analysis. First, the 2 mm of Δ can be used as a minimum prerequisite to recognize the beginning of convective cloud development. Then, the progress of charge separation strongly influences the development of lightning can be detected when the value of the Δ maintained with at least 2 mm with the minimum period of three consecutive hours. From these criteria, about 69% of the samples with the minimum Δ of 2 mm were the lightning days and the rest was no lightning. Second, the average period of lightning development was about six hours. In nowcasting, the longer period means more time for safety preparation. Third, the average of Δ with the lightning event was higher of 1.64 mm and 0.23 mm compared to the overall sample and fair weather condition, respectively. This generally showed that the PWV content was highly unstable compared during the fair weather.

The ability of GPS PWV to nowcast the lightning activities during the 2009 inter-monsoons were demonstrated through the changes of Δ . On average, the lightning in the study area was typically started after 6 hours from the first of 2 mm with an average of 3.64 mm. This scenario was also observed during the lightning days between 07:00 LT and 22:00 LT. The finding shows a very significant result that can be proposed as an alternative method to nowcasting the lightning activity using the GPS PWV data. With the advancement of GPS technology and the spreading of the GPS network around the world, the deployment of this method is promising and cost-effective. However, the results mentioned above were only limited to the inter-monsoons season in 2009 (May and November). To maximize the benefits, these findings need to be strengthened by conducting a further research such as for the condition out of the inter-monsoons period as well as covering a few years of data.

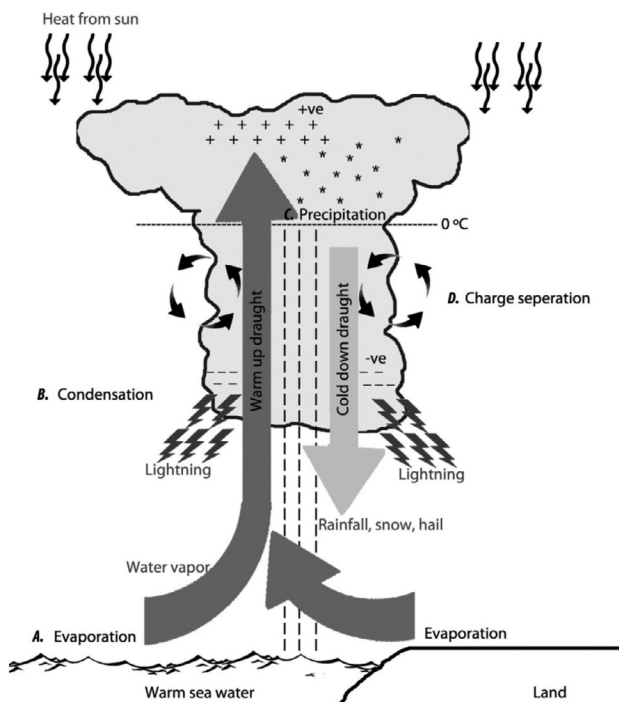


Figure 12. The water evolution and the process involved. The mechanism process started from the evaporation (labeled as A) until charge separation (labeled as D).

Acknowledgements. This research was supported under UKM-GGPM-ICT-122-2010 grant. The second author is a PhD student supported by the Universiti Pertahanan Nasional Malaysia (UPNM). The authors would like to thank the Department of Irrigation and Drainage Malaysia (DIDM) for providing the rainfall data, the Malaysia Meteorology Department (MMD) for lightning and meteorological data as well as the Department of Survey and Mapping Malaysia (DSMM) for supporting the GPS data.

References

- Altamimi, Z., P. Sillard and C. Boucher (2002). ITRF2000: A new release of the international terrestrial reference frame for Earth science applications, *J. Geophys. Res.*, 107 (B10), 2214; doi:10.1029/2001JB000561.
- Backer, M.B., A.M. Blyth, H.J. Christian, A.M. Gadian, J. Latham and K. Miller (1999). Relationship between lightning activity and various thundercloud parameters: satellite and modeling studies, *Atmos. Res.*, 51, 221-236.
- Coster, A.J., A.E. Niell, F.S. Solheim, V.B. Mendes, P.C. Toor, K.P. Buchmann and C.A. Upham (1996). Measurements of Precipitable Water Vapor by GPS, Radiosondes, and a Microwave Water Vapor Radiometer, In: Proceedings of the 9th International Technical Meeting of the Satellite Division of The Institute of Navigation (ION GPS 1996), Kansas City, MO, September 1996, 625-634.
- El-Rabbany, A. (2002). Introduction to GPS: The Global Positioning System, Artec House Inc., Boston/London.
- Garner, T.W., T.L. Gaussiran, B.W. Tolmana, R.B. Harris, R.S. Calfas and H. Gallagher (2008). Total electron content measurements in ionospheric physics, *Adv. Space Res.*, 42, 720-726.
- Ge, M., E. Calais and J. Haase (2000). Reducing satellite orbit error effects in near real-time GPS zenith tropospheric delay estimation for meteorology, *Geophys. Res. Lett.*, 1915-1918; doi:10.1029/1999GL011256.
- Hay, C., and J. Wong (2000). Enhancing GPS: Tropospheric Delay Prediction at Master Control Station, *GPS World*, 11, 56-62.
- Inoue, H.Y., and T. Inoue (2007). Characteristics of the Water-Vapor Field over the Kanto District associated with summer thunderstorm activities, *SOLA*, 3, 101-104.
- Nakamura, H. (2003). International workshop on GPS meteorology, http://dbx.cr.chiba-u.jp/Gps_Met/gpsmet/CD-1_Proceedings_PDF/01_Head/01_08_WsSummary.pdf.
- Price, C. (2000). Evidence for a link between global lightning activity and upper tropospheric water vapor, *Nature*, 406, 290-293.
- Rocken, C., T. Van. Hove and R. Ware (1997). Near real-time sensing of atmospheric water vapor, *Geophys. Res. Lett.*, 24, 3221-3224.
- Suparta, W., Z.A. Abdul. Rashid, M.A. Mohd. Ali, B. Yatim and G.J. Fraser (2008). Observations of Antarctic precipitable water vapor and its response to the solar activity based on GPS sensing, *J. Atmos. Sol.-Terr. Phys.*, 70, 1419-1447.
- Suparta, W., J. Adnan and M.A. Mohd. Ali (2011). Detection of lightning activity using GPS PWV measurements, In: Proceedings of the 2011 IEEE International Conference of Space Science and Communication (IconSpace), July 12-13, IEEE Xplore Press, Penang, 115-120.
- Suparta, W., A. Iskandar, M.S.J. Singh, M.A. Mohd. Ali, B. Yatim and A.N.M. Yatim (2013). Analysis of GPS water vapor variability during the 2011 La Niña event over the western Pacific Ocean, *Annals of Geophysics*, 56 (3), R0330; doi:10.4401/ag-6261.
- Williams, E. (2003). Charge structure and geographical variation of thunderclouds, In: V. Cooray (ed.), *The Lightning Flash*, The Institution of Engineering and Technology, London, United Kingdom.
- Ziegler, C.L., D.R. MacGorman, P.S. Ray and J.E. Dye (1991). A model evaluation of noninductive graupel-ice charging in the early electrification of a mountain thunderstorm, *J. Geophys. Res.*, 96, 12833-12855.
- Zipser, E.J. (1994). Deep cumulonimbus cloud system in the tropics with and without lightning, *Weather Rev.*, 122, 1837-1851.
- Zipser, E.J., and K. Lutz (1994). The vertical profile of radar reflectivity of convective cells: a strong indicator of storm intensity and lightning probability?, *Mon. Weather Rev.*, 122, 1751-1759.

*Corresponding author: Wayan Suparta, Universiti Kebangsaan Malaysia, Space Science Centre (ANGKASA), Institute of Climate Change, Selangor, Malaysia; email: wayan@ukm.edu.my.